Preliminary Assessment of Optimal Longitudinal-Mode Control for Drag Reduction through Distributed Aeroelastic Shaping

Corey Ippolito[1] and Nhan Nguyen[2]
NASA Ames Research Center, Moffett Field, CA 94035

Jason Lohn[3]
Carnegie Mellon University in Silicon Valley, Moffett Field, CA 94035

and

John Dolan[4]
Carnegie Mellon University, Pittsburgh, PA

The emergence of advanced lightweight materials is resulting in a new generation of lighter, flexible, more-efficient airframes that are enabling concepts for active aeroelastic wing-shape control to achieve greater flight efficiency and increased safety margins. These elastically shaped aircraft concepts require non-traditional methods for large-scale multi-objective flight control that simultaneously seek to gain aerodynamic efficiency in terms of drag reduction while performing traditional command-tracking tasks as part of a complete guidance and navigation solution. This paper presents results from a preliminary study of a notional multi-objective control law for an aeroelastic flexible-wing aircraft controlled through distributed continuous leading and trailing edge control surface actuators. This preliminary study develops and analyzes a multi-objective control law derived from optimal linear quadratic methods on a longitudinal vehicle dynamics model with coupled aeroelastic dynamics. The controller tracks commanded attack-angle while minimizing drag and controlling wing twist and bend. This paper presents an overview of the elastic aircraft concept, outlines the coupled vehicle model, presents the preliminary control law formulation and implementation, presents results from simulation, provides analysis, and concludes by identifying possible future areas for research.

I. Introduction

Continuing advances in modern engineered materials and the need for greater efficiency of aircraft in flight are driving new aircraft design concepts that incorporate lightweight flexible multi-functional structures. These new structural concepts provide less rigidity while maintaining the same load-carrying capacity as previous generation designs. The Boeing 787 Dreamliner aircraft's highly flexible wing structure is an example of this emerging trend. These advances are also driving research into active aeroelastic shape control of these flexible aircraft structures during flight. For instance, elastically shaping an aircraft by actively controlling wing wash-out twist and wing bending deflection in order to change the local angle of attack has the potential to yield lower fuel burn by drag reduction during cruise. Structural flexibility can further be leveraged to realize a revolutionary, optimal wing shape design that can accommodate a significant curvature for drag reduction benefits.

A conceptual study was recently conducted outlining the concept for Adaptive Aeroelastic Shape Control (AASC)[1]. This study outlines plans for multi-disciplinary design, analysis and optimization to examine the potential

---

[1] Research Scientist, Intelligent Systems Division, NASA Ames Research Center. AIAA Member
[2] Research Scientist, Intelligent Systems Division, NASA Ames Research Center. AIAA Associate Fellow
[3] Associate Research Professor, Carnegie Mellon University Silicon Valley, Moffett Field, CA
[4] Senior Systems Scientist, Robotics Institute, Carnegie Mellon University, Pittsburgh, PA

American Institute of Aeronautics and Astronautics

benefits of AASC on a flexible aircraft in flight over a conventional aircraft with traditional flight control system design.

Four major technical areas of AASC research were outlined in this study:

1. Vehicle concept design and optimization
2. Aeroelastic flight dynamic modeling
3. Elastically wing shaping actuation design
4. Flight control design and vehicle simulation

Significant research activity has occurred on the AASC in several of these areas, including a distributed actuation system for effecting elastic shape control [2], investigation of non-linear coupling between aeroelastic modes and the flight vehicle dynamics [3], development of a coupled high-fidelity numerical model utilizing vortex-lattice and finite-element methods [4], offline shape optimization studies for drag minimization [5,6], and development of a lower-order aeroelastic vehicle model that is appropriate for control law development [7].

This study builds on results from this previous research and focuses on flight control design in technical area 4 above. Research under this area seeks to develop multi-objective flight control to simultaneously gain aerodynamic efficiency while maintaining traditional pilot command-tracking tasks for guidance and navigation. Research in this area also seeks to develop guidance laws to achieve low drag objectives, with specific focus on cruise segment of flight, applying modern multi-objective optimal control techniques for control of elastically-shaped aircraft.

This paper presents a preliminary study of a notional multi-objective control law for an elastically-shaped flexible-wing aircraft with distributed leading and trailing edge control surface actuators. The purpose of this initial study is to determine feasibility of a centralized control framework that simultaneously minimizes drag, stabilizes structural modes, and simultaneously performs longitudinal attack-angle command-tracking tasks. This initial study continues the previous research by implementing the proposed control concept [7], utilizing distributed control surface actuation for control of the coupled aeroelastic and flight dynamics model. This study develops a multi-objective control structure in a standard unconstrained linear-quadratic optimization framework and implements this controller on the recently developed model. The goals of this initial study are to demonstrate feasibility of this approach using a preliminary control concept, provide an assessment of expected performance improvements, identify challenges, and outline directions for future research to enable large-scale multi-objective control of aeroelastically shaped vehicles.

This paper is organized as follows. The concept for elastically-shaped aircraft is presented, followed by a coupled aeroelastic flight dynamics model on which this work is based. The optimal control problem is formalized, the solution is presented, and the simulation implementation is presented. The closed-loop response of the system is presented with a focus on estimating quantifiable performance benefits. The results will be discussed, limitations identified, and a directions for future work are presented.

II. Elastically Shaped Aircraft Model

The model[4] utilized in this study describes the longitudinal dynamics of a generic transport aircraft at Mach 0.80 and Mach 0.88 at an altitude of 35,000 ft. The longitudinal dynamics are described by two aircraft states: angle of attack α and pitch rate q. The aircraft model contains 80 structural states capturing the 20 dominant flexible modes, and provides 23 control inputs: one elevator, 11 flaps, and 11 slats; as shown in Figure 1.
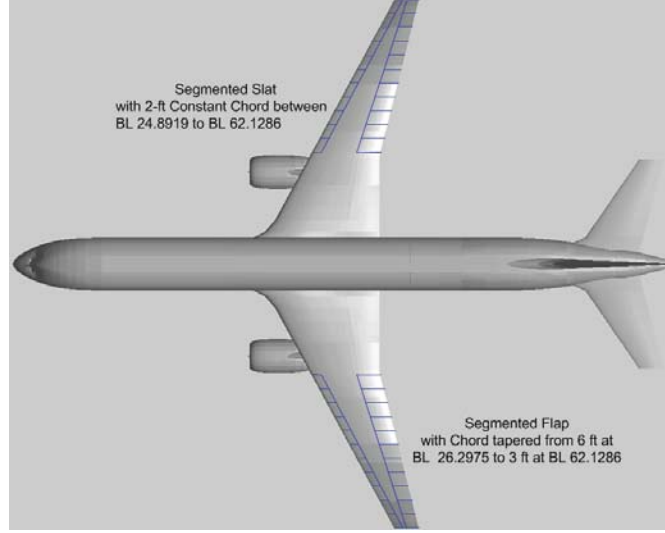
American Institute of Aeronautics and Astronautics

Figure 1. Distributed leading-edge (slats) and trailing-edges (flaps) actuator configuration.

The coupled equations of motion are given by

$$\begin{bmatrix} \dot{x}_r \\ \dot{x}_e \end{bmatrix} = \begin{bmatrix} A_{rr} & A_{re} \\ A_{er} & A_{ee} \end{bmatrix} \begin{bmatrix} x_r \\ x_e \end{bmatrix} + \begin{bmatrix} B_{rr} & B_{re} \\ B_{er} & B_{ee} \end{bmatrix} \begin{bmatrix} u_r \\ u_e \end{bmatrix}$$

(1)

where the states are given by $x_r = [\alpha \quad q]^T$, $x_e = [q_w \quad q_\theta \quad \dot{q}_w \quad \dot{q}_\theta]^T$, and $q_w, q_\theta \in \mathbb{R}^m$ are the generalized coordinate vectors for bending and torsion, respectively, along with their derivatives $\dot{q}_w, \dot{q}_\theta \in \mathbb{R}^m$. The elements of q_w and q_θ are indexed such that q_{w_i} and q_{θ_i} are the wing bending and torsional deflections of mode i = 1,…,m, where m=20 is the total number of mode shapes. The input $u_r = [\delta_e]$ is the elevator flap deflection angle, and $u_e = [\delta_f \quad \delta_s]^T$ where δ_f is the vector of 11 distributed flap inputs and δ_s are the 11 distributed slat input. This results in a model with 82 states and 23 inputs. This initial study assumes all aeroelastic modes and vehicle states are observable.

The lift and drag characteristics of the aircraft are functions of the current vehicle states, flexible-mode states, and control inputs as described by the following equations

$$\Delta C_D = K(2C_L \Delta C_L + \Delta C_L^2) + C_{D_u} u + C_{D_{u^2}} u^2$$
$$C_L = C_{L_0} + \Delta C_L$$
$$\Delta C_L = C_{L_x} x + C_{L_u} u$$

(2)

where K is the drag polar parameter, C_D is the total drag coefficient, and C_L is the total lift coefficient.

III. Control Law Formulation

The control system is designed using full-state feedback with the addition of tracking error integral feedback as developed in the literature [4] and summarized below. The controller tracks a reference angle of attack signal, α_c. An integrator state x_α integrates the attack angle error signal for feedback, given by

$$\dot{x}_\alpha = A_\alpha (\alpha_r - \alpha_c)$$

(3)

where A_α is the integrator gain, and can be combined with the system in (1) to form an augmented system for control development. The final augmented system is then of the form

$$\dot{x} = Ax + Bu + z$$
$$y = Cx + Du$$

(4)

where $x \in \mathbb{R}^N$ is of size N=83 and $u \in \mathbb{R}^M$ is of size M=23, given by

$$x = [x_r \; x_e \; x_a]^T \; ; \; u = [u_r \; u_e]^T$$

$$A = \begin{bmatrix} A_{rr} & A_{re} & 0 \\ A_{er} & A_{ee} & 0 \\ [A_a \; 0] & 0 & 0 \end{bmatrix} \; ; \; B = \begin{bmatrix} B_{rr} & B_{re} \\ B_{er} & B_{ee} \\ 0 & 0 \end{bmatrix} \; ; \; z = \begin{bmatrix} 0 \\ 0 \\ -A_a x_{r_{ref}} \end{bmatrix} \; ; \; C = I \; ; \; D = 0$$

(5)

3

The feedback control cost function J includes quadratic costs terms to address the multiple control objectives.

$$J(x,u,t) = \frac{1}{2}\int_0^\infty (x^T Q x + u^T R u + k_d C_D) dt \tag{6}$$

The weighting matrix $Q = diag\{Q_r, Q_e, Q_\alpha\}, Q > 0$ and its submatrices are diagonal matrices to achieve tracking of the vehicle states x_r, control of the aeroelastic states x_e, and the α command tracking integral, respectively. Similarly, $R = diag\{R_f, R_s, R_e\}, R > 0$ and its submatrices penalize control actuation effort of the flaps, slats, and elevator, respectively. Total drag C_D term with a scalar weight $k_d > 0$. Substituting C_D into J yields

$$\begin{aligned} J(x,u,t) = \frac{1}{2}\int_0^\infty & \left(x^T Q x + u^T R u + k_d C_{D_0} + k_d K \left(C_{L_0} + C_{L_x} x + C_{L_u} u \right)^2 + k_d C_{D_u} u \right. \\ & \left. + u^T k_D diag \left(C_{D_{u^2}} \right) u \right) dt \end{aligned} \tag{7}$$

The control solution for problems of this form[7] is given by

$$u(x,z) = u_x x + u_z z + u_c \tag{8}$$

where

$$\begin{aligned} u_x &= -\bar{R}^{-1}\left(B^T P + q_d K C_{L_u}^T C_{L_x}\right) \\ u_z &= -(\bar{R}^{-1}B^T S) \\ u_c &= -\bar{R}^{-1}\left(q_d K C_{L_u}^T C_{L_0} + \frac{1}{2}q_d C_{D_u}^T + B^T \lambda_0\right) \end{aligned} \tag{9}$$

The value of P is found from the solution to the following algebraic Riccati equation

$$P\bar{A} + \bar{A}^T P - PB\bar{R}^{-1}B^T P + \bar{Q} = 0 \tag{10}$$

where

$$\begin{aligned} \bar{R} &= R + q_d K C_{L_u}^T C_{L_u} + q_d C_{D_{u^2}} \\ \bar{A} &= A - B\bar{R}^{-1}q_d K C_{L_u}^T C_{L_x} \\ \bar{Q} &= Q + q_d K C_{L_x}^T \left(C_{L_x} - C_{L_u}\bar{R}^{-1}q_d K C_{L_u}^T C_{L_x}\right) \end{aligned} \tag{11}$$

and

$$S = (PB\bar{R}^{-1}B^T - \bar{A}^T)^{-1}P$$
$$\lambda_0 = (PB\bar{R}^{-1}B^T - \bar{A}^T)^{-1}\left(q_d K C_{L_x}^T C_{L_0} - (PB + q_d K C_{L_x}^T C_{L_u})\bar{R}^{-1}\left(q_d K C_{L_u}^T C_{L_0} + \frac{1}{2}q_d C_{D_u}^T\right)\right) \tag{12}$$

The sufficient condition for a solution to exist requires checking the following, from which $\bar{Q} > 0$ can be implied.

$$k_d K C_{L_u}^T C_{L_x} < \bar{R} \tag{13}$$

IV. Implementation

Forming the closed loop system of (4) under the feedback law (8), and noting that $z = -A_a v \alpha_c$ where $v = [0 \dots 0\ 1]^T$, yields

$$\begin{aligned} \dot{x} &= (A + Bu_x)x - A_a(Bu_z + I)v(\alpha_c) \\ u &= u_x x - A_a u_z v \alpha_c + u_c \\ y &= x \end{aligned} \tag{14}$$

Without loss of generality the constant term Bu_c has been dropped from the derivative equation in (14), noting that this term results in an offset x_s of the state vector, which is given by

$$\tilde{x} = x + x_s$$
$$x_s = A^{-1}B\bar{R}^{-1}\left(q_d K C_{L_u}^T C_{L_0} + \frac{1}{2}q_d C_{D_u}^T + B^T \lambda_0\right) \tag{15}$$

4

where $\tilde{x}$ is the complete solution state vector. Also note that equation (15) can be solved using the original system matrix $\begin{bmatrix} A_{rr} & A_{re} \\ A_{er} & A_{ee} \end{bmatrix}$, which is invertible, and the effect of the constant u_c term in the integrator can be solved separately.

For evaluation of total drag, we define a total drag metric which integrates C_D over the specified time interval.

$$C_{D_{avg}} = \frac{1}{t_f} \int_0^{t_f} \Delta C_D dt \tag{16}$$

The state and aeroelastic weighting matrices were initially selected based on Bryson's criteria, which sets the initial weighting elements based on the maximum expected value of the state and input elements. The Q and R diagonal matrices are given by

$$Q_r = k_{qr} \cdot diag\left[\frac{1}{\alpha_{max}^2}, \frac{1}{q_{max}^2}\right]$$

$$Q_e = k_{qe} \cdot diag\left[1/q_{w_{max}}^2 \quad 1/q_{\theta_{max}}^2 \quad 1/\dot{q}_{w_{max}}^2 \quad 1/\dot{q}_{\theta_{max}}^2\right]$$

$$Q_a = k_{qa}$$

$$R_r = k_{re} \cdot \left[\frac{1}{\delta_{e_{max}}^2}\right]$$

$$R_e = diag\left\{k_{rf} \cdot diag\left[\frac{1}{maxexp(u_{e_i})^2}\right], k_{rs} \cdot diag\left[\frac{1}{maxexp(u_{e_i})^2}\right]\right\} \tag{17}$$

The scalar parameter set $k = \{k_d, k_{qr}, k_{qe}, k_{qa}, k_{re}, k_{rs}, k_{rf}\}$ allows for tuning of relative weights in the cost function as permissible, subject to the conditions in (13).

V. Results

Evaluation of the open loop models for both Mach 0.80 and Mach 0.88 shows that the two models are similar in structure and have unstable open-loop modes, but the both pairs $(\bar{A}, B)$ are controllable and the unstable modes can be stabilized through LQR feedback, as exemplified in Figure 2.
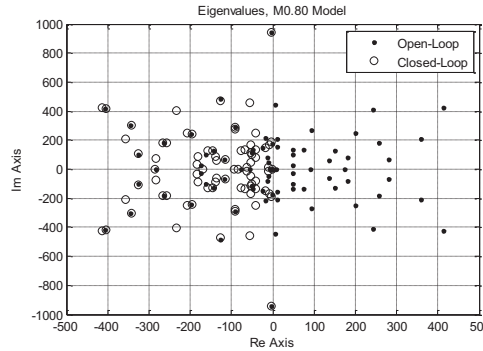

Figure 2. Open-loop and closed-loop poles. *Shown for Mach 0.80 model under uniform feedback, the closed-loop system poles are all in the left-hand plane.*

A. Step-Response Study Results

The model and controller were implemented in Matlab for evaluation. To evaluate the control effectiveness and drag reduction efficacy, the results were compared against a single-objective attack angle tracking controller, which was approximated by setting the state tracking error to a large value and setting the rest of the weight factors to a small value. The following tests show simulation response of the closed-loop system to a step control signal input of $\alpha_c = 5.0°$ over a 15 second interval.

For the baseline comparison approximating single-objective control, the controller was derived with aircraft state tracking gain k_{qr}=10, and all other k-gain scaling factors set to k=0.01. The resulting response is shown in Figure 3. The baseline controller results in a C_{Davg}=1.058e5 over the 15 second interval. The integrator winds up based on initial

5

error to the step response; since the integrator has a low weighting, the wind-up has a small effect on the response and results in a slow wind-down. The initial system response to the step disturbance is a strong initial control surface response that quickly stabilizes.

Emphasizing drag-reduction in the control law is achieved by setting the drag weighting scale factor (kd=1e4) higher than the remaining gains (all other gains set to 1.0), except the integrator feedback gain was set to a low value to be ignored by the control law (kqa=1e-5). This results in the response shown Figure 4, with a drag reduction of 93.8% from the baseline (CDavg reduced from 1.058e5 to 6.476e3).

Including drag-reduction with state-tracking objectives (kd=kqr=1e2) while minimizing other objectives (k=1e-5) results in the response shown in Figure 5. The resulting drag CDavg=6.518e3, which is greater than an order of magnitude improvement over the baseline CDavg=1.058e5 (a 93.8% decrease). Figure 6 shows the result of further increasing the drag gain (kd=1e8, kqr=1e3, all other k=1e-5) to the point where numerical issues begin to arise in the Matlab solver at the default precision. This results in a CDavg=5.531e3 (a 94.8% drag metric reduction from the baseline) but worse tracking performance.

Figure 7 shows step response when integrator-performance objectives are added to the overall cost function in addition to drag-reduction and state-tracking (kd=kqr=kqa=1e2), while minimizing other objectives (k=1e-5). Note that the inclusion of the integrator in this structure and in response to a large step input disturbance contributes to overshoot in the attack angle response.

Emphasizing aeroelastic-control objectives, in addition to drag-reduction and state-tracking objectives, results in the response shown in Figure 8. The resulting drag CDavg=1.1o71e5 is slightly higher than the baseline CDavg=1.058e5. However, the flaps and slats have a more active response with larger required deflections.

The results in Figure 8 show a large drag response and large actuator deflections, which can be addressed through increasing the drag-reduction objective gain (kd=1e3) and the control cost gains (kre=krs=krf=1), while keeping vehicle state and aeroelastic control objectives the same (kqr=kqe=1). The results in Figure 9 show the effect of this modification, with a 71% relative reduction in drag (from CDavg=1.171e5 to CDavg=3.332e4) and a significantly reduced actuator magnitude response.

Equally considering all objectives by setting all k gains uniformly to 1 yields the results in Figure 10. The resulting drag CDavg=2.013e5 has increased from the baseline due to balanced demands. An undesirable integrator wind-up is observed, which occurs over the first 2.5 seconds followed by a slow wind down, and the integrator response contributes to the overshoot and a low-amplitude low-frequency oscillatory response.
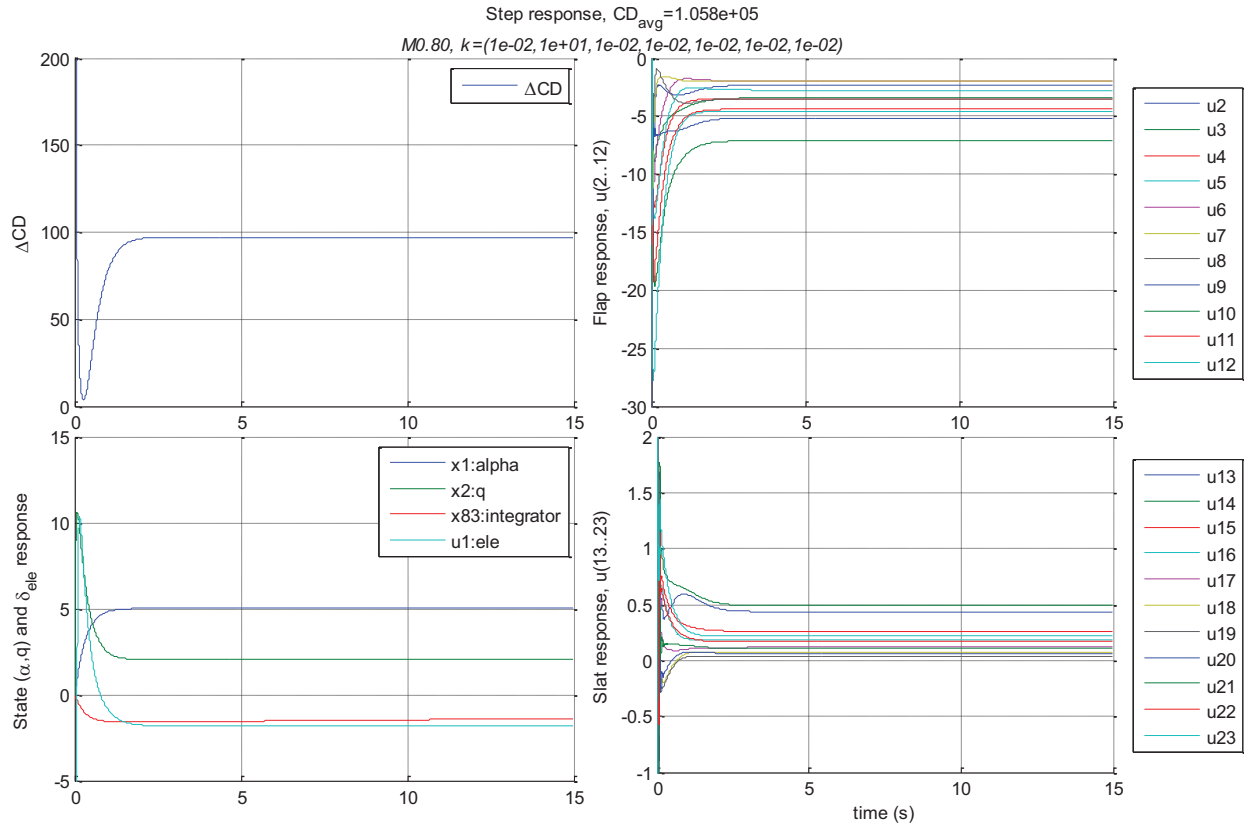
American Institute of Aeronautics and Astronautics

Step response, CD$_{avg}$=1.058e+05

M0.80, k=(1e-02,1e+01,1e-02,1e-02,1e-02,1e-02,1e-02)

Figure 3. Baseline step response, state tracking objective.

Step response, TotCD=6.476e+03

M0.80, k=(1e+04,1e+00,1e+00,1e-05,1e+00,1e+00,1e+00)
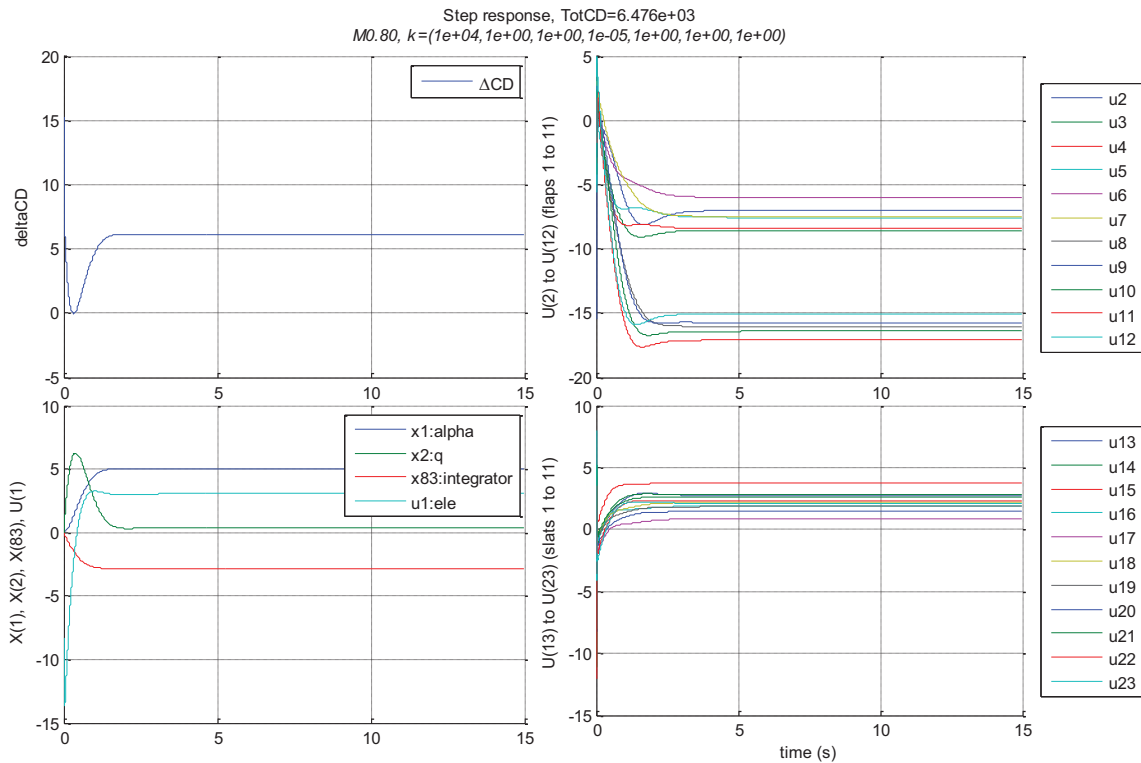
Figure 4. Step response with drag reduction prioritized.

7

American Institute of Aeronautics and Astronautics

Step response, CD$_{avg}$=6.518e+03

M0.80, k=(1e+02,1e+02,1e-05,1e-05,1e-05,1e-05,1e-05)
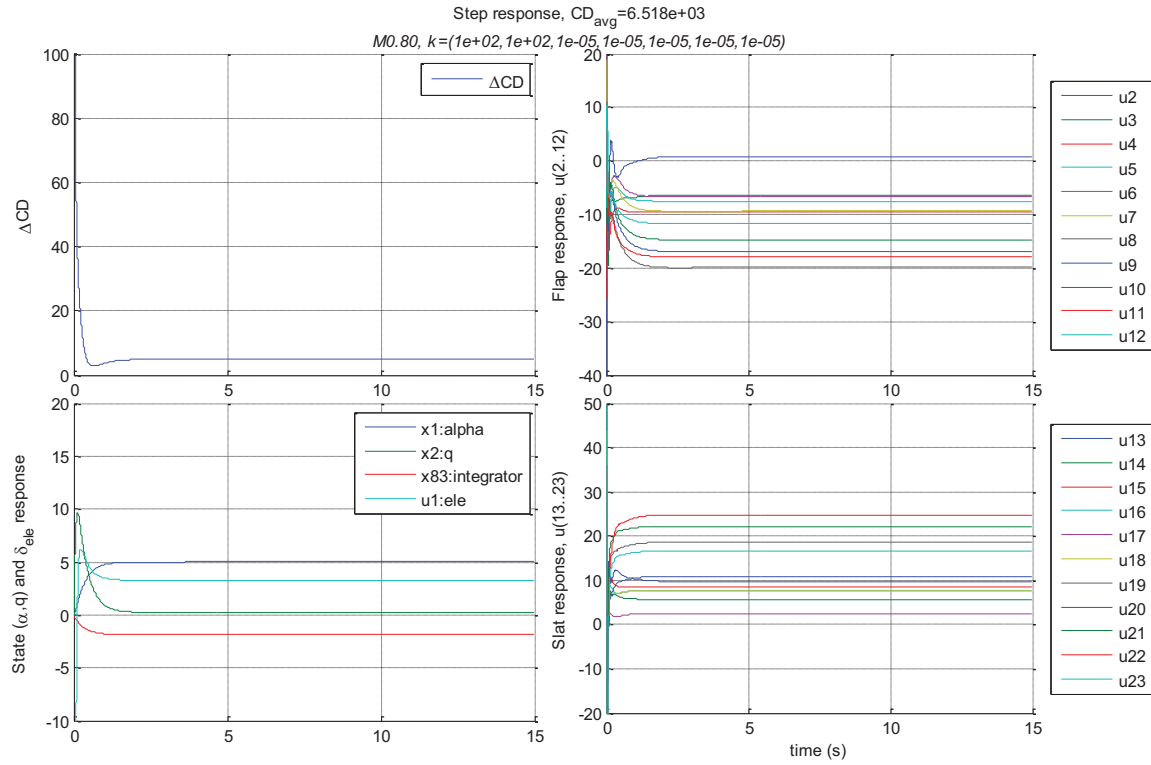
Figure 5. Step response, emphasized drag-reduction and state-tracking objectives.

Step response, CD$_{avg}$=5.531e+03

M0.80, k=(1e+08,1e+03,1e-05,1e-05,1e-05,1e-05,1e-05)
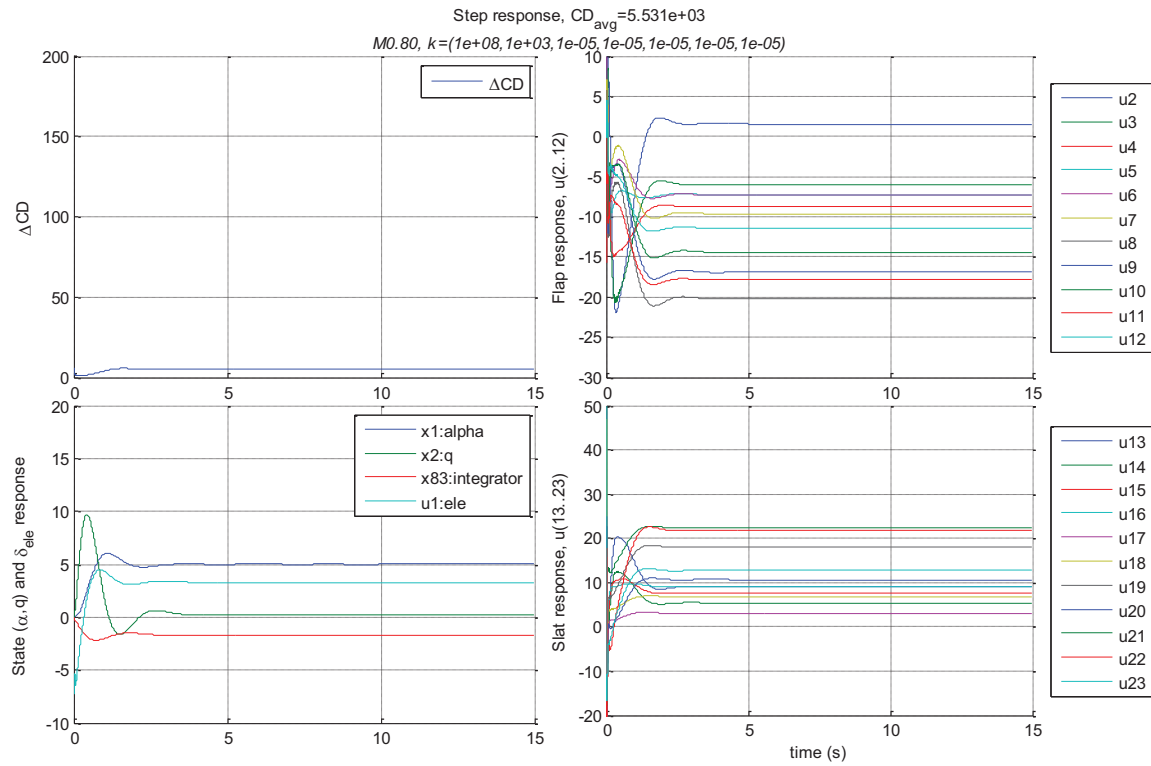
Figure 6. Step response, further increasing drag cost gain relative to state-tracking.

8

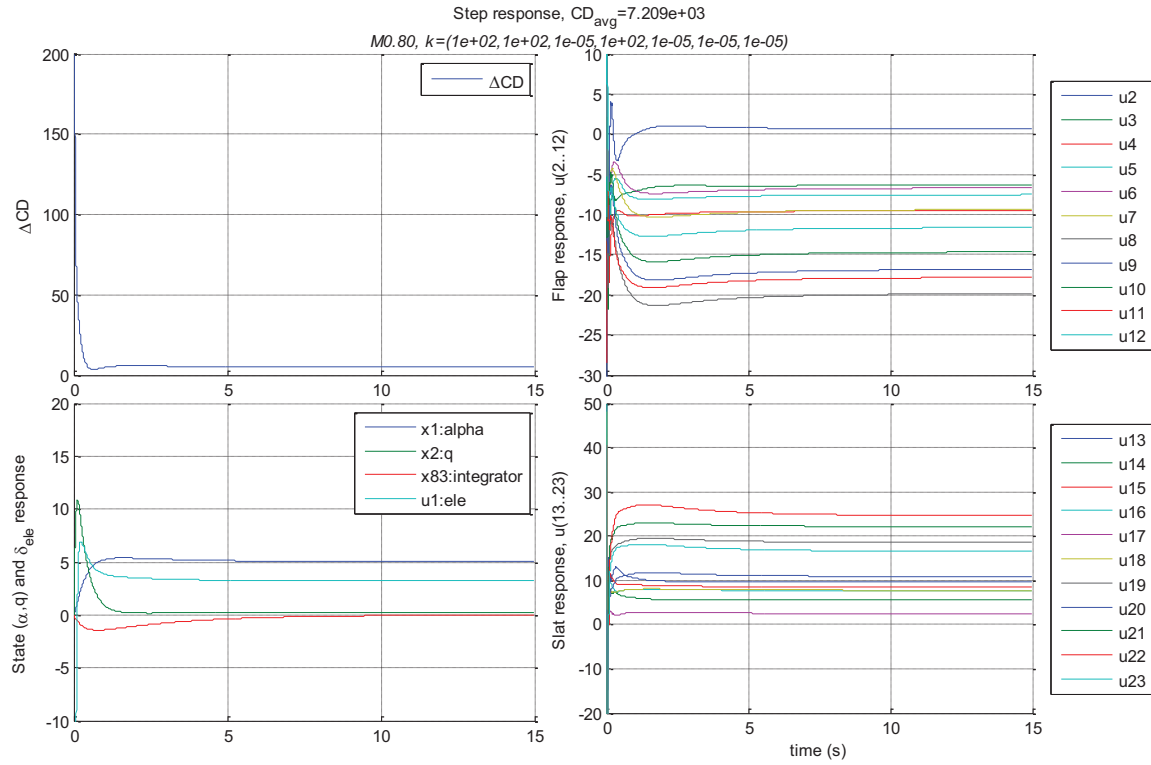American Institute of Aeronautics and Astronautics

Figure 7. Step response with emphasized state-tracking, drag-reduction, integrator performance.
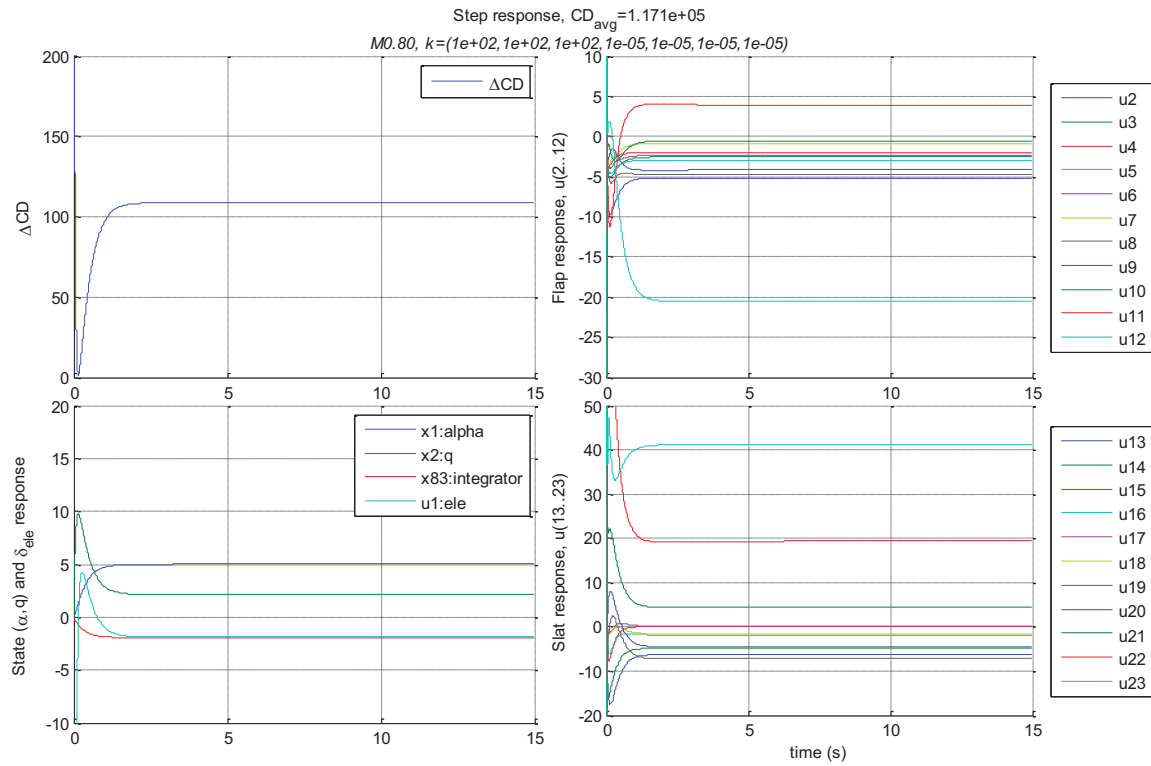
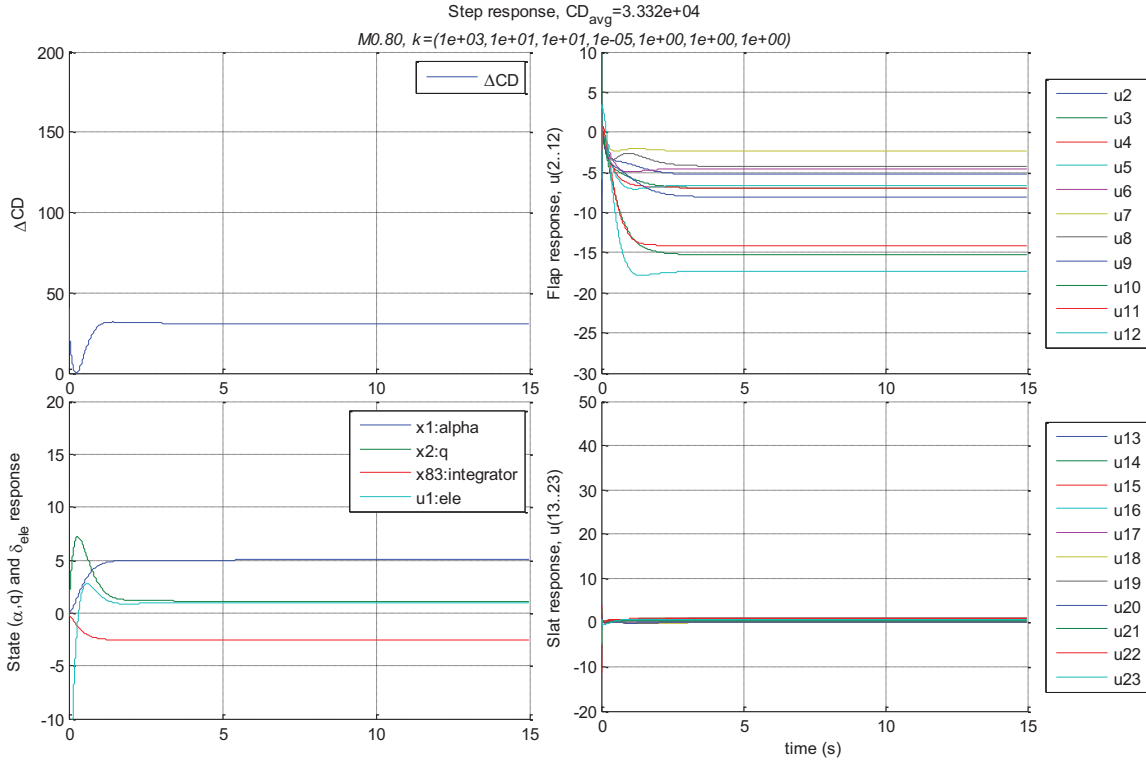**Figure 8. Step response with aeroelastic-control, drag, and state-tracking objectives.**

American Institute of Aeronautics and Astronautics

Step response, CD_avg=3.332e+04

M0.80, k=(1e+03,1e+01,1e+01,1e-05,1e+00,1e+00,1e+00)

Figure 9. Step response with drag reduction actuator objectives

Step response, CD_avg=2.013e+05

M0.80, k=(1e+00,1e+00,1e+00,1e+00,1e+00,1e+00,1e+00)
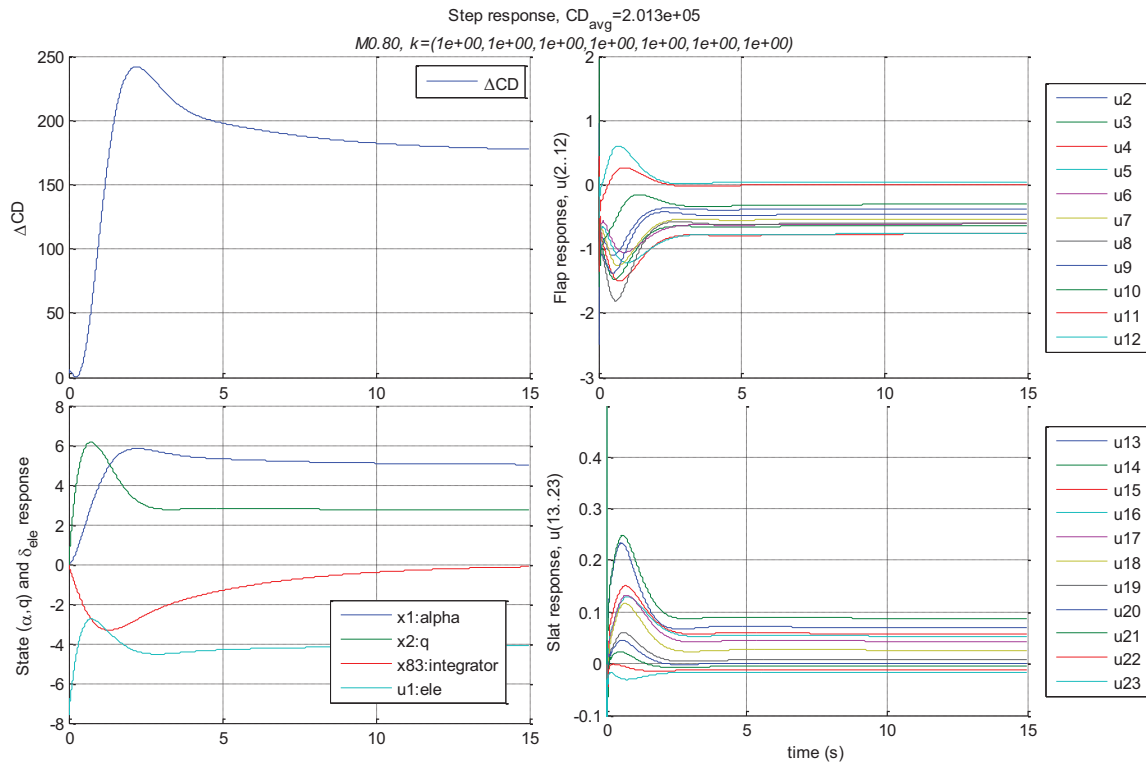
Figure 10. Step response with equally weighted objectives.

American Institute of Aeronautics and Astronautics

VI. Conclusion

The purpose of this initial study was to demonstrate feasibility of multi-objective drag-minimizing control for a flexible-wing aircraft with distributed actuators through a linear-quadratic control optimization framework, demonstrate an initial implementation based on the recently derived models, provide an assessment of expected performance improvements, and identify limitations and goals for future development of this system. The design and implementation of the control system presented in this initial study showed promising results. The multi-objective controller saw significant drag improvements as compared to the baseline single-objective controller. The controller was relatively straight-forward to derive and the solution was readily computationally-solvable. Incorporation of high-level control gains in the control structure allowed intuitive adjustments to be made to the closed-loop system response. Inclusion of the integrator structure was likewise easy to accomplish, and suggests further structural modifications to the controller will not be problematic.

The results highlighted issues that will need to be addressed in further iterations of the control structure. In the preliminary control structure presented, response of the control surfaces are unconstrained, allowing large deflections, ignoring relative constraints between actuators, and allowing immediate response. The gains for tuning controller response provide a coarse mechanism to limit actuator response within a desired range. However, the control formulation should be rederived as a constrained control problem to formally address these issues and assess for robustness. A number of integrator issues were observed in the response of this preliminary control structure, many of which can be corrected through the addition of a model reference filter to produce an achievable and smoothly varying α_c based on the plant dynamics, and further overshoot issues can be addressed through augmenting the feedback structure, such as adding derivative feedback paths. Once the structure of the controller has been finalized, an optimization methodology would facilitate gain selection for real-world implementation. The aircraft model used in this study is linearized; the effect of non-linear uncertainty may be of importance to consider. Direct sensing of all aeroelastic states will not be likely possible, and observer designs may be considered. Drag optimization in this study was based on an idealized drag polar, and methods for directly estimating and controlling drag may be necessary for achieving minimal drag on higher-fidelity models. Once these issues are addressed, future research will investigate integration into a larger control design framework, including extending control to handle speed and lateral modes, and integration with outer-loop control structures or guidance trajectories signals. Multi-objective trajectory optimization can be utilized to provide additional drag minimizing benefits, and trajectory-based control strategies[8] may be utilized to help improve tracking performance. Incorporating the wing-shape control targets found from offline optimization studies on the higher-fidelity numerical AASC model[5] should provide additional drag benefits. Finally, this controller and guidance and navigation solutions will be implemented and tested against the high-fidelity models and higher-fidelity vehicle simulators that are currently in development.

Acknowledgments

References

[1] Nguyen, N. "NASA Innovation Fund 2010 Project: Elastically Shaped Future Air Vehicle Concept," NASA Internal Report

[2] Urnes, J., Nguyen, N., Ippolito, C., Totah, J., Trinh, K., and Ting, E. "A Mission Adaptive Variable Camber Flap Control System to Optimize High Lift and Cruise Lift to Drag Ratios of Future N+3 Transport Aircraft" 51st AIAA Aerospace Sciences Meeting, Grapevine, TX, January 2013

[3] Nguyen, N., Trinh, K., Nguyen, D., Tuzcu, I., "Nonlinear Aeroelasticity of Flexible Wing Structure Coupled with Aircraft Flight Dynamics," AIAA Structures, Structural Dynamics, and Materials Conference, AIAA-2012-1792, April 2012.

[4] Nhan T. Nguyen, Eric B. Ting, Daniel Nguyen, Tung Dao, and Khanh T. "Coupled Vortex-Lattice Flight Dynamic Model with Aeroelastic Finite-Element Model of Flexible Wing Transport Aircraft with Variable Camber Continuous Trailing Edge Flap for Drag Reduction", AIAA Atmospheric Flight Mechanics (AFM) Conference. August 2013

[5] Ippolito, C., Nguyen, N., Totah, J., Trinh, K., Ting, E. "Initial Assessment of a Variable-Camber Continuous Trailing-Edge Flap System on a Rigid Wing for Drag Reduction in Subsonic Cruise" AIAA Infotech@Aerospace (I@A) Conference, August 19-22, 2013, Boston, MA

[6] Nguyen, N., Trinh, K., Reynolds, K., Kless, J., Aftosmis, M., Urnes, J. "Elastically Shaped Wing Optimization and Aircraft Concept for Improved Cruise Efficiency" AIAA Paper 2013, Vol 141, 2013

[7] Nguyen, N., Urnes, J. "Aeroelastic Modeling of Elastically Shaped Aircraft Concept via Wing Shaping Control for Drag Reduction". AIAA Atmospheric Flight Mechanics Conference. 13 - 16 August 2012, Minneapolis, Minnesota

American Institute of Aeronautics and Astronautics

[8]Adami, T., Zhu, J., Ishihara, A., Yeh, Y., Ippolito, C. "Six-DOF trajectory tracking for payload directed flight using trajectory linearization control". Proc. of AIAA Guidance, Navigation and Control Conference, Seattle, Washington. Pg 1897-1916. 2009

American Institute of Aeronautics and Astronautics